Soft Matter

Effect of Dynamically Heterogeneous Interphases on Particle Dynamics of Polymer Nanocomposites

Journal:	*Soft Matter*
Manuscript ID	SM-ART-12-2022-001617.R2
Article Type:	Paper
Date Submitted by the Author:	23-Feb-2023
Complete List of Authors:	Wu, Di; Stevens Institute of Technology, Chemical Engineering and Materials Science Narayanan, Suresh; Argonne National Laboratory Advanced Photon Source Li, Ruhao; Stevens Institute of Technology, Chemical Engineering & Materials Science Feng, Yi; Stevens Institute of Technology, Chemical Engineering and Materials Science Akcora, Pinar; Stevens Institute of Technology, Chemical Engineering and Materials Science

Effect of Dynamically Heterogeneous Interphases on Particle Dynamics of Polymer Nanocomposites

Di Wu[†], Suresh Narayanan[§], Ruhao Li[†], Yi Feng[†] and Pinar Akcora[†,*]

[†]Department of Chemical Engineering and Materials Science, Stevens Institute of Technology, Hoboken, New Jersey 07030, United States

[§]Advanced Photon Source, Argonne National Laboratory, Lemont, Illinois 60439, United States

[*]Corresponding author

Abstract

The entanglements of dynamically asymmetric polymer layers influence relaxations of nanoparticles in polymer nanocomposites. In this work, dynamics of polymer-adsorbed and polymer-grafted nanoparticles in poly(methyl acrylate) matrix polymer was investigated using X-ray photon correlation spectroscopy (XPCS) to understand the role of chain rigidity and chemical heterogeneities on particle dynamics. Location of dynamic heterogeneities close to nanoparticles and away from particle surfaces were examined with the comparison of adsorbed and grafted nanoparticles. Our results show that the chemical heterogeneities around dispersed nanoparticles transitioned the particle dynamics from Brownian diffusion into hyperdiffusion, and moreover, the high rigidity of chains in the chemically heterogeneous interfacial layers slowed down the particle dynamics. The hyperdiffusion measured both in grafted particles and adsorbed particles was attributed to the dense interfacial mixing of dynamically heterogeneous chains.

1. Introduction

Functionalizing nanoparticles through chain adsorption or grafted nanoparticles is a common strategy to control particle dispersion in polymer nanocomposites and their structure, dynamics and mechanical properties have been extensively investigated[1-19]. Relating the particle dynamics to the dynamics of polymer grafted chains has significant importance in understanding the composite dynamics, however it can only be attained for matrix-free composites. The recent simulation study on grafted particles in unentangled matrix showed that relaxations of monomers close to particle surfaces are slower than the chains farther away due to graft chain constraints and the confinement of neighbor chains[20]. This heterogeneity of relaxations around nanoparticles perturbs particle motions. At short times, particles behave in a sub-diffusive manner and for long times they follow Fickian diffusion[20]. For grafted particle composites with entangled matrix chains, dynamics of the grafted particle is affected by the interfacial interactions between graft and matrix chains[21, 22]. Thus, the strength of these interactions depends on the chemistry and lengths of graft and matrix chains, creating weak and strong interphase layers of varying entanglement densities[22, 23].

The polymer-particle interphases govern the dynamics of both the fillers and matrix polymer. Dynamics of nanoparticles in polymers contributes to our understanding on the viscosity changes and reinforcement origin of nanocomposites, and on the relaxations of host polymers depending on particle-polymer interactions[16, 24-29]. X-ray photon correlation spectroscopy (XPCS) probes nanoparticle dynamics in viscoelastic media, and directly measures nanoparticle relaxations in highly entangled polymer melt[30-33]. Entanglement controlled environment such as the high-molecular-weight solutions was shown to dictate the temporal fluctuations of the entanglement mesh[34]. This environmental restriction controls the sub-diffusive motion of nanoparticles. Another

mode of dynamics measured in various systems is hyperdiffusion. This mode of particle dynamics seen in colloidal gels, soft materials and colloidal polycrystals are related to non-equilibrium events or attributed to the stresses built upon deformation or to the mechanical and dynamic responses of materials to internal stresses[35-38]. In this study, we aim to understand the effect of polymer dynamical asymmetry on dynamics of composite systems with bare particles and grafted nanoparticles using XPCS and rheology.

We studied rheological properties and chain dynamics of polymer nanocomposites with asymmetric interphases in previous works. The amorphous, and weakly interacting polymer blends in the presence of nanoparticles reversibly stiffened at high temperatures due to dynamic heterogeneities, arising from the mixing and interpenetration of chemically different adsorbed and matrix chains[39, 40]. Thus, dynamic heterogeneities rely on the chain conformations and are highly dependent on the confinement of neighboring chains. The dynamic coupling between the two polymers with different glass-transition temperatures (T_g's) was found to strengthen the composite as a result of slowed chain dynamics when all chains were mobile at high temperatures[40, 41]. The matrix chain length and the adsorbed chain rigidity were found to affect this dynamic coupling process[22, 42,23]. For example, local viscosities measured by magnetic heating of iron oxide nanoparticles were directly influenced by the rigidity of adsorbed polymers and chemical heterogeneities of their interfacial layers[43]. In another work, we reported that particles adsorbed with the highly mobile short chains moved faster since the short chains can dilate the highly dense (entangled) environment around the particles[22]. The highly mobile short chains mix and entangle with the matrix polymer in the interphase layer and this factor governs the hyperdiffusive motion[22]. Dynamics of grafted particles was shown to depend on particle dispersion[21]. Well dispersed grafted particles were found to be diffusive, and upon large shear deformation dynamics transitioned to

hyperdiffusion. This change in particle dynamics was associated with the enhanced entanglements between grafted and matrix chains and to the free volume available within particles at low graft density[21].

This work focuses on exploring the effect of interfacial stresses on hyperdiffusion. This dynamic mode was observed in many polymer nanocomposites[22, 32, 37, 44-46]. In some systems, hyperdiffusion was attributed to the stresses that could arise when chains were thermally non-equilibrated[36, 47]. The systems investigated here deals with the stresses created in two poly(methyl acrylate) (PMA) nanocomposites with particles adsorbed or grafted with chemically different polymer chains. We will discuss the particle dynamics in these composites at the same loading (10 vol%). The entanglement states, dynamic heterogeneities, and free volume within the interfacial layers differ in our samples. The particle dynamics and rheology results are affected by the rigidity and molecular weight of chains, which are in fact related to the chain entanglement and free volume in the system. We prepared PMA (40 kDa) composites consisting of PMMA-, PVAc- and P2VP-adsorbed (listed in the order of increasing rigidity) Fe_3O_4 and silica (SiO_2) (15-nm) nanoparticles and the PMMA-grafted Fe_3O_4 (15-nm) nanoparticles. These composites with two different dispersion states are discussed to understand the particle relaxations. Overall, XPCS data of the three systems collected at 140 °C are presented along with particle dispersion, rigidity of interfacial chains and matrix molecular weight.

2. Experimental section

Adsorption of polymers onto nanoparticles and preparation of polymer-grafted Fe_3O_4 nanoparticles were reported in previous works[23, 41]. Here, we will describe the preparation of polymer adsorbed SiO_2 nanoparticles. SiO_2 in butanone with 15-nm diameter were purchased from Nissan Chemical Corporation. 400 mg of NPs were mixed with 45 mL of deionized (DI) equimolar water/ethanol mixture in a 100 mL two-neck flask. Colloidal solution was stirred under continuous nitrogen flow for one hour. Then, the solution was bath-sonicated for another 30 min. 0.8 mL of (3-aminopropyl)triethoxysilane (APTES), purchased from Sigma Aldrich, was added to the nanoparticle solution and the reaction was let to proceed at 40 ºC under nitrogen for 12 h. Amine functionalized nanoparticles were collected after centrifuging and washed with acetone and DI water three times. PMMA (35 kDa), with a polydispersity index of 1.1 was synthesized via atom transfer radical polymerization (ATRP) in our laboratory. The concentration of the polymer solution was kept constant at 15 mg/mL for all samples. Amine functionalized SiO_2 was added to the polymer solution at a particle concentration of 5 mg/mL in acetonitrile for PVAc and PMMA, in dichlorobenzene for P2VP. Solution was then sonicated for 10 min and stirred for another 30 min. Polymer adsorbed nanoparticles were collected by centrifugation and washed with corresponding solvent several times to remove all free residual polymers. The particles were dried again under vacuum at room temperature. The number of adsorbed chain density per SiO_2 nanoparticle is calculated using TGA data shown in **Figure S1**. TGA data of Fe_3O_4 samples was reported in previous work[23]. The characteristic ratios (C_∞)[41, 48] and the amounts of adsorbed polymers (as mass percent and as number of chains per nanoparticle) and their molecular weights are summarized in **Table 1**.

Table 1. Adsorbed or grafted chain density of particles and the characteristic ratio (C_∞) of the adsorbed or grafted polymer used in decorating the nanoparticles. 40 kDa PMA is used as matrix in all composites. Grafted particle composites have 20 and 160 kDa PMA matrix.

Composites	Chain density (chains/nm^2)	C_∞
35 kDa PMMA-ads-SiO_2	0.004	7
50 kDa PVAc-ads-SiO_2	0.007	9
40 kDa P2VP-ads-SiO_2	0.013	10
35 kDa PMMA-ads-Fe_3O_4	0.035	7
50 kDa PVAc-ads-Fe_3O_4	0.005	9
40 kDa P2VP-ads-Fe_3O_4	0.010	10
148 kDa PMMA-gr- Fe_3O_4/ 20/160 kDa PMA	0.045	7

Preparation of Nanocomposites

PMA was dissolved in acetonitrile to form a solution with 15 mg/mL concentration. Polymer-adsorbed NPs were added to the PMA solution to achieve a nanoparticle concentration of 10 vol% particle core. After sonicating and shaking for 30 min, the solution was cast into Teflon cups, and the solvent was let to evaporate at room temperature. The films were dried in vacuum oven at 130 ºC for 3 days to remove all residual solvent. Samples were then molded into disks with 8-mm diameter and 0.8-mm height for rheological tests. The molded disks were annealed at 180 ºC in vacuum oven prior to rheology tests.

Transmission Electron Microscope (TEM)

Polymer adsorbed NH_2-Fe_3O_4 PMA composites were cryomicrotomed and then imaged in JEOL USA JEM-2100Plus Transmission Electron Microscope operated at 200 kV and equipped with a cold-field emission gun.

Rheology Experiments

Linear viscoelastic data of polymer nanocomposite melts was measured in ARES-G2 strain-controlled rheometer using 8-mm parallel plates. Time-Temperature Superposition (TTS) curves were obtained for a wide frequency range measured at 35, 55, 85 and 140 °C. The reference temperature of 35 °C was above the glass-transition temperature of PMA ($T_{g,PMA}$:15 °C).

X-ray Photon Correlation Spectroscopy (XPCS)

XPCS measurements were performed at the 8-ID-I beamline of the Advanced Photon Source (APS) at Argonne National Laboratory. Sample areas of 15 μm × 15 μm were illuminated by coherent X-rays with photon energy of 11 keV. The normalized intensity−intensity autocorrelation function was obtained over the wave vector range 0.027 $nm^{-1} < q < 0.1$ nm^{-1}. Samples were held at the desired temperature for 20 min for thermal equilibrium prior to the measurement. Data were collected at five different locations for each sample to ensure uniformity and stability of the particle dispersion.

3. Results and Discussion

The autocorrelation functions for all XPCS experiments performed at 140 °C were analyzed by the Siegert relation: $g_2(q,t) = 1 + B\ exp\left[-2(t/\tau(q))^{\beta}\right] + \Delta$. $\tau(q)$ is the characteristic relaxation time of particle, β is the stretching exponent, B is the instrument dependent Siegert factor, q is the scattering vector and Δ is the baseline correction term. In our previous study, a strongly confined particle diffusion was found in the PMMA adsorbed Fe_3O_4 nanoparticles as measured with the larger local viscosity and the smaller diffusivity compared to the more rigid PVAc and P2VP chains[23]. SAXS and TEM results indicated similar aggregations (~100 nm) in all the samples (**Figure S2**). The particle dynamics of the samples is presented in **Figure 1**. The strong interfacial interactions between PMA matrix chains and flexible adsorbed chains are expected to slow down the particle dynamics. As seen, the particles adsorbed with PMMA are the slowest, and with P2VP is the fastest (**Figure 1a**). The strong interphase formation was observed in rheology measurements, where the reinforcement of PMMA adsorbed particles is higher than the composites with weak interphases in the case of P2VP and PVAc[23]. The bare particles exhibit slower relaxations than the PVAc adsorbed particles since PMA is strongly adsorbed on particles. All samples exhibited hyperdiffusion with $\tau \sim q^{-1}$ (**Figure 1b**). The q dependent stretching exponent β falls within 1 to 2 which is typical for hyperdiffusion (**Figure 1c**).

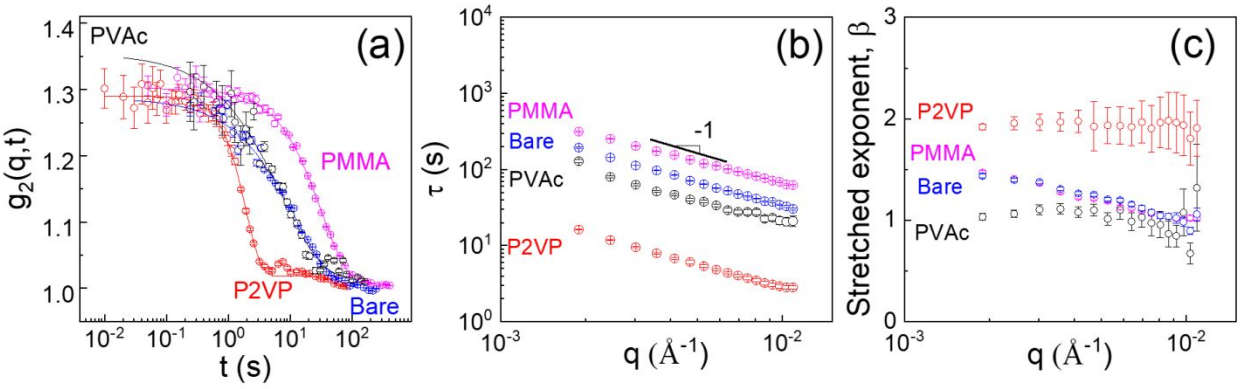

Figure 1. (a) Autocorrelation functions, $g_2(q, t)$, for the 35 kDa PMMA, 50 kDa PVAc, 40 kDa P2VP adsorbed and bare 15-nm Fe_3O_4 nanoparticles in 40 kDa PMA matrix at q=0.01 $Å^{-1}$ and 140 ^oC. The solid lines are the stretched exponential model fits. **(b)** Relaxation times and **(c)** stretched exponents as a function of q for the corresponding samples. Particle loading is 10 vol%.

We prepared another system of PMA-SiO_2 composites to evaluate the role of particle dispersion on particle dynamics. Similar adsorbed chain types and molecular weights and the PMA matrix polymer were used in preparation of this composite system. Particle dispersion in PMA-SiO_2 composites is investigated via SAXS and TEM. SAXS data is analyzed by multi-level unified function analysis[49]. The primary size of the SiO_2 particles is found from the first level fitting as $R_{g,1}$~10 nm. The scattering signal of bare 15-nm SiO_2 nanoparticles in 40 kDa PMA showed a clear Guinier plateau at low q, indicating a good dispersion of particles, was also confirmed by its TEM data (**Figure 2**). The upturn at low $q < 0.002$ $Å^{-1}$ is associated with a small number of large aggregates. With the higher rigidity of adsorbed (P2VP) chains, SiO_2 particles were found to be aggregated. The number of levels used in the Unified model fitting to the data may not be as reliable to interpret the aggregate sizes and clusters (**Table S1**). TEM data helps to explain the SAXS data analysis from the multi-level unified model fittings. As seen, particles are more aggregated with the rigid P2VP adsorbed chains.

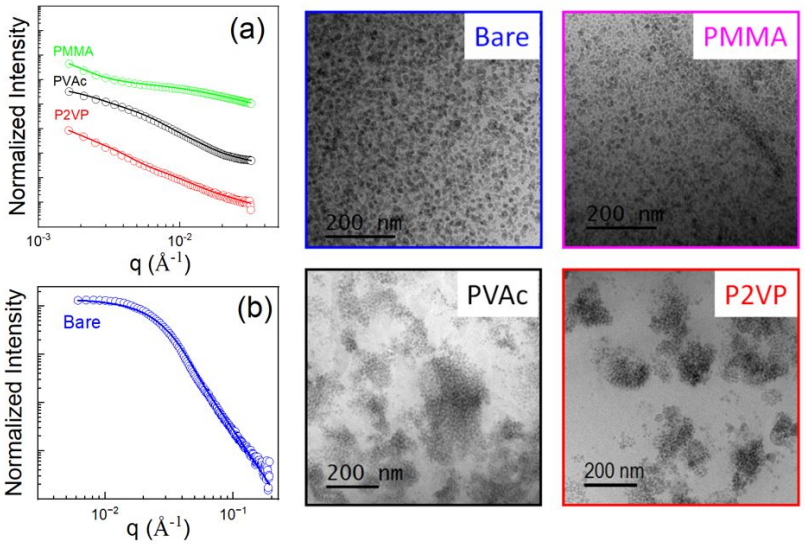

Figure 2. Small angle X-ray scattering (SAXS) and TEM data for the **(a)** 35 kDa PMMA, 50 kDa PVAc, and 40 kDa P2VP adsorbed and **(b)** bare 15-nm SiO_2 particles in 40 kDa PMA matrix. Solid lines on SAXS profiles are the Unified model fittings. Particle loading is 10 vol% in all samples.

Different particle dispersion of SiO_2-PMA allowed us to discuss the linear viscoelastic behavior and particle dynamics with the observed structures. In previous work, the rubber plateau modulus (G_N) of Fe_3O_4-PMA composites with similar particle dispersion was found to decrease when the entanglements of the interfacial layers were primarily weakened by the more rigid adsorbed polymer as shown in **Figure 3a**. In SiO_2-PMA composites, G_N increased with the adsorbed chain rigidity. The rigidity of interfacial layers improves the mechanical properties of SiO_2-PMA, contrary to what was measured in Fe_3O_4-PMA. The comparison of rheology data indicates that modulus enhancement in SiO_2-PMA was dominated by particle aggregation, but not directly related to the entanglement densities deduced from the rheology data. **Figure 3b** shows that entanglement density (Z) in PMMA and P2VP with SiO_2 fillers is almost the same, but it decreased

from 19 to 7 with the Fe_3O_4 system. It is important to note that the adsorbed chain density (in chains/nm^2) of the same polymer on both SiO_2 and Fe_3O_4 fillers are close in value (**Table 1**). The zero-shear viscosity of PMA-SiO_2 composite was found to be higher than the bare composite (**Figure 3c**). The rise of zero-shear viscosity at low frequency for PMA-SiO_2 composites with the P2VP and PVAc chains indicates the aggregation state of particles.

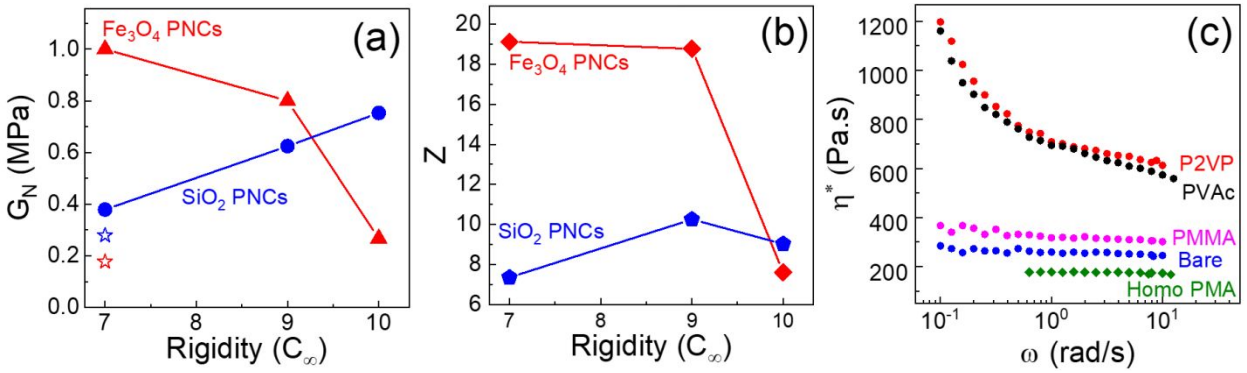

Figure 3. Comparison of **(a)** rubbery plateau modulus (G_N) and **(b)** entanglement density ($Z=\sqrt[3]{\left(\frac{\tau_d}{\tau_e}\right)}$) ($\tau_e$ is the entanglement relaxation time and τ_d is the terminal relaxation time) for the PMMA, P2VP, PVAc adsorbed SiO_2 and Fe_3O_4 nanoparticle PMA composites with 10 vol% loading. Open stars are for the bare Fe_3O_4 and SiO_2 PMA composites. Data of Fe_3O_4 system is reproduced from *J. Appl. Phys.* 2021, *130* (6), 064701 with the permission of AIP Publishing. **(c)** Complex viscosities in terminal regions of SiO_2 nanocomposites with bare, 35 kDa PMMA, 50 kDa PVAc, 40 kDa P2VP adsorbed particles at 10 vol% loading in 40 kDa PMA matrix measured at 140 °C.

Knowing the structural and rheological behavior of SiO_2 composites, herein we discuss their XPCS data. For bare composite, the particles are found to diffuse in a Brownian mode with $\tau \sim q^{-2}$ and the stretching exponent β is stable and close to 1 (**Figures 4a-c**). The relaxation of particles adsorbed with PVAc and P2VP is so slow that the autocorrelation functions do not fully decay (**Figure 4a**).

Relaxation times of the strongly aggregated PVAc and P2VP samples exhibited a q-independent behavior (**Figure 4b**). The restricted motions in PVAc and P2VP samples are seen with their constant relaxations across the q-range. A slight decrease in relaxation of PVAc composite is seen at low-q region, but it remains unchanged within the high q-range. For PMMA-adsorbed sample, hyperdiffusive behavior was observed. This transition indicates the effect of dynamic heterogeneity, shifting the dynamics from Brownian diffusion to hyperdiffusion (**Figure 4b**). A similar transition was observed when matrix molecular weight increased from 2 kDa to 280 kDa[50]. The decline of β from 2 to 1 was attributed to structural heterogeneities of aggregates (**Figure 4c**). Particles moved faster both in the well-dispersed bare and PMMA samples compared to the aggregated particles as in P2VP and PVAc as particle mobility was restricted by neighboring particles within a cluster. The slower mobility of PMMA sample than that of the bare sample was directly associated with the interphase effect. Weak interphases with the PVAc and P2VP experience more dynamic heterogeneities (β >1) compared to the PMMA sample with strong interphases (β <1). The hyperdiffusive character of PMMA system is attributed to the coupling of the particles with center-of-mass motion of polymer (segmental relaxations) as was presented in previous work[51, 52]. Hyperdiffusive behavior of PMMA system with β <1 is a transitional dynamics which may related to the internal dynamic stresses built within PMMA-PMA interfacial layers.

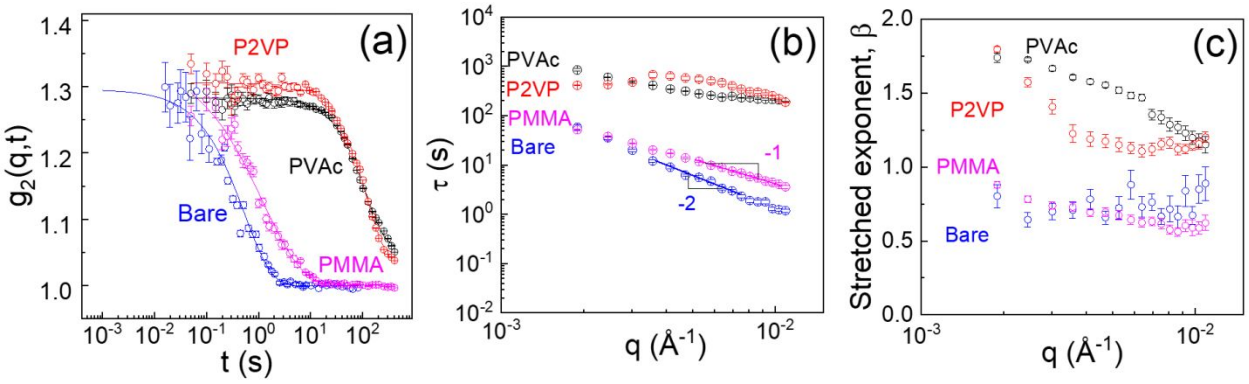

Figure 4. (a) Autocorrelation function, $g_2(q, t)$, for bare SiO_2 particle, 35 kDa PMMA, 50 kDa PVAc, and 40 kDa P2VP adsorbed SiO_2 nanoparticle in 40 kDa PMA at 140 ^oC and q=0.01 $Å^{-1}$. The solid lines are the stretched exponential fits. **(b)** Particle relaxations and **(c)** stretched exponent, β, versus q. Particle loading is 10 vol%.

We have discussed the effects of adsorbed polymer rigidity and particle dispersion on particle relaxations. Next, we seek to understand the dynamics of grafted nanoparticle composites. The interfacial mixing of grafted and matrix chains and entanglements are very different because chain topologies and entropic mixing are different in grafted systems depending on the grafting density and graft length. Grafted Fe_3O_4 particle relaxations would be influenced with interfacial chain heterogeneity and mixing. It is worth to mention that rheological properties of the grafted composites were tested and reported in our previous work[41]. We found that short matrix chains dynamically couple better with the long-grafted chains and reinforce the system at high temperatures. Here, we will present the relaxations of PMMA-grafted Fe_3O_4 (15-nm) nanoparticles in 20 kDa and 160 kDa PMA matrix. The grafting density is 0.045 chains/nm^2, molecular weight of PMMA graft chains is 148 kDa. The particles moved surprisingly faster in 160 kDa PMA matrix than those in 20 kDa PMA (**Figures 5a-b**). A clear hyperdiffusive motion is measured for both

matrix molecular weights, and β falls within 1 and 1.5 (**Figure 5c**). The observed slow mobility of grafted particles in 20 kDa PMA is explained by the low friction of short matrix chains diffusing into the grafted chains and forming a denser interfacial layer. This dense layer effect was verified by the higher reinforcement observed with the short (20 kDa) PMA chains in our previous work[41].

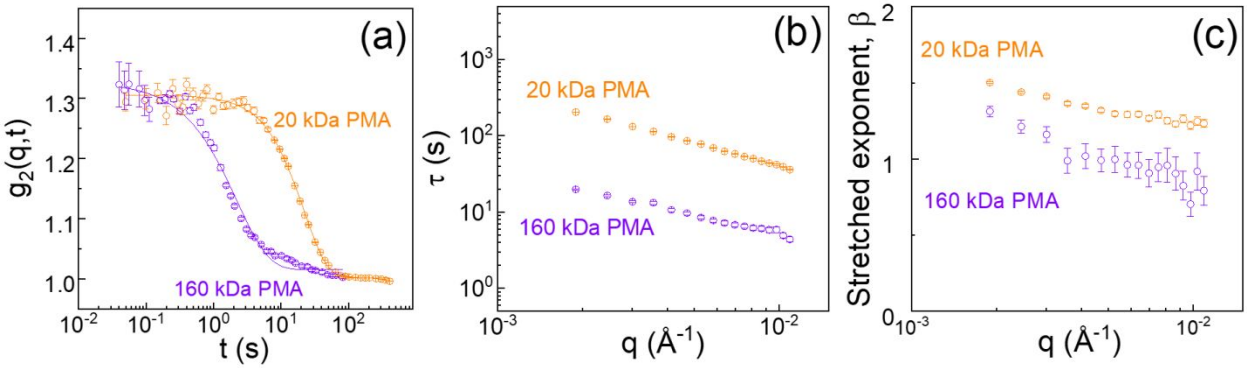

Figure 5. (a) Autocorrelation functions, $g_2(q, t)$, for 148 kDa PMMA-grafted 15-nm Fe_3O_4 nanoparticles in 20 kDa and 160 kDa PMA matrix at 140 °C and q=0.01 Å^{-1}. The lines are the stretched exponential fittings. **(b)** Particle relaxation times and **(c)** stretched exponents versus q for the same composites. Particle loading is 10 vol%.

4. Conclusion

The particle relaxations in three different PMA nanocomposite systems are discussed. Results show that in aggregated Fe_3O_4 particles with the flexible PMMA adsorbed chains, the particle relaxation is slower than the particles decorated with the more rigid, PVAc and P2VP chains. In well-dispersed bare SiO_2 composites, the free diffusion of particles in an entangled matrix was measured. A transition from Brownian diffusion to hyperdiffusion was observed for samples with dynamic heterogeneities in their interfacial layers. Specifically, low rigidity of chains in interfacial

regions creates the denser layers of chains around nanoparticles and builds up internal stresses within, where chemically different dynamically asymmetric chains are mixed. The hyperdiffusion measured in these composites is explained by the internal stress heterogeneities between chemically different polymers. This study uses grafted and adsorbed nanoparticles as model systems to understand the proximity of spatial heterogeneities, chain rigidity and entanglement effects on particle dynamics. Overall, the rigidity of chains controls the entanglement density, the packing of chains and presumably the free volume within entanglements and these factors influence the particle dynamics, which have implications on the use of nanocomposites for membrane applications.

Conflicts of interest

There are no conflicts to declare.

Acknowledgements

We acknowledge funding from the National Science Foundation Grant CMMI MEP #1825250, and the US Department of Energy through the Argonne National Laboratory under Grant No. DE-AC02-06CH11257.

References

1. Du, F.; Scogna, R. C.; Zhou, W.; Brand, S.; Fischer, J. E.; Winey, K. I., Nanotube networks in polymer nanocomposites: Rheology and electrical conductivity. *Macromolecules* **2004,** *37* (24), 9048-9055.

2. Kumar, S. K.; Benicewicz, B. C.; Vaia, R. A.; Winey, K. I., 50th Anniversary Perspective: Are Polymer Nanocomposites Practical for Applications? *Macromolecules* **2017,** *50* (3), 714-731.

3. Jancar, J.; Douglas, J. F.; Starr, F. W.; Kumar, S. K.; Cassagnau, P.; Lesser, A. J.; Sternstein, S. S.; Buehler, M. J., Current issues in research on structure-property relationships in polymer nanocomposites. *Polymer* **2010,** *51* (15), 3321-3343.

4. Carrillo, J. M. Y.; Cheng, S.; Kumar, R.; Goswami, M.; Sokolov, A. P.; Sumpter, B. G., Untangling the Effects of Chain Rigidity on the Structure and Dynamics of Strongly Adsorbed Polymer Melts. *Macromolecules* **2015,** *48* (12), 4207-4219.

5. Merabia, S.; Sotta, P.; Long, D. R., A microscopic model for the reinforcement and the nonlinear behavior of filled elastomers and thermoplastic elastomers (Payne and Mullins Effects). *Macromolecules* **2008,** *41* (21), 8252-8266.

6. Meera, A. P.; Said, S.; Grohens, Y.; Thomas, S., Nonlinear viscoelastic behavior of silica-filled natural rubber nanocomposites. *Journal of Physical Chemistry C* **2009,** *113* (42), 17997-18002.

7. Akcora, P.; Kumar, S. K.; Moll, J.; Lewis, S.; Schadler, L. S.; Li, Y.; Benicewicz, B. C.; Sandy, A.; Narayanan, S.; Ilavsky, J.; Thiyagarajan, P.; Colby, R. H.; Douglas, J. F., "Gel-like" mechanical reinforcement in polymer nanocomposite melts. *Macromolecules* **2010,** *43* (2), 1003-1010.

8. Akcora, P.; Kumar, S. K.; García Sakai, V.; Li, Y.; Benicewicz, B. C.; Schadler, L. S., Segmental dynamics in PMMA-grafted nanoparticle composites. *Macromolecules* **2010,** *43* (19), 8275-8281.

9. Khan, J.; Harton, S. E.; Akcora, P.; Benicewicz, B. C.; Kumar, S. K., Polymer crystallization in nanocomposites: spatial reorganization of nanoparticles. *Macromolecules* **2009,** *42* (15), 5741-5744.

10. Senses, E.; Jiao, Y.; Akcora, P., Modulating interfacial attraction of polymer-grafted nanoparticles in melts under shear. *Soft Matter* **2014,** *10* (25), 4464-4470.

11. Winey, K. I.; Vaia, R. A., Polymer nanocomposites. *MRS Bulletin* **2007,** *32* (4), 314-319.

12. Mu, M.; Composto, R. J.; Clarke, N.; Winey, K. I., Minimum in diffusion coefficient with increasing MWCNT concentration requires tracer molecules to be larger than nanotubes. *Macromolecules* **2009,** *42* (21), 8365-8369.

13. Kumar, S. K.; Jimenez, A. M., Polymer adsorption-reversible or irreversible? *Soft Matter* **2020,** *16* (23), 5346-5347.

14. Jouault, N.; Moll, J. F.; Meng, D.; Windsor, K.; Ramcharan, S.; Kearney, C.; Kumar, S. K., Bound polymer layer in nanocomposites. *ACS Macro Letters* **2013,** *2* (5), 371-374.

15. Trazkovich, A. J.; Wendt, M. F.; Hall, L. M., Effect of Copolymer Sequence on Local Viscoelastic Properties near a Nanoparticle. *Macromolecules* **2019,** *52* (2), 513-527.

16. Bailey, E. J.; Winey, K. I., Dynamics of polymer segments, polymer chains, and nanoparticles in polymer nanocomposite melts: A review. *Progress in Polymer Science* **2020,** *105*, 101242.

17. Power, A. J.; Papananou, H.; Rissanou, A. N.; Labardi, M.; Chrissopoulou, K.; Harmandaris, V.; Anastasiadis, S. H., Dynamics of Polymer Chains in Poly(ethylene oxide)/Silica Nanocomposites via a Combined Computational and Experimental Approach. *Journal of Physical Chemistry B* **2022,** *126* (39), 7745-7760.

18. Modica, K. J.; Martin, T. B.; Jayaraman, A., Effect of Polymer Architecture on the Structure and Interactions of Polymer Grafted Particles: Theory and Simulations. *Macromolecules* **2017,** *50* (12), 4854-4866.

19. Cheng, S.; Carroll, B.; Lu, W.; Fan, F.; Carrillo, J. M. Y.; Martin, H.; Holt, A. P.; Kang, N. G.; Bocharova, V.; Mays, J. W.; Sumpter, B. G.; Dadmun, M.; Sokolov, A. P., Interfacial Properties of Polymer Nanocomposites: Role of Chain Rigidity and Dynamic Heterogeneity Length Scale. *Macromolecules* **2017,** *50* (6), 2397-2406.

20. Chen, Y.; Xu, H.; Ma, Y.; Liu, J.; Zhang, L., Diffusion of polymer-grafted nanoparticles with dynamical fluctuations in unentangled polymer melts. *Physical Chemistry Chemical Physics* **2022**.

21. Liu, S.; Senses, E.; Jiao, Y.; Narayanan, S.; Akcora, P., Structure and Entanglement Factors on Dynamics of Polymer-Grafted Nanoparticles. *ACS Macro Letters* **2016,** *5* (5), 569-573.

22. Yang, S.; Liu, S.; Narayanan, S.; Zhang, C.; Akcora, P., Chemical heterogeneity in interfacial layers of polymer nanocomposites. *Soft Matter* **2018,** *14* (23), 4784-4791.

23. Wu, D.; Feng, Y.; Li, R.; Ozisik, R.; Akcora, P., Entanglement density and particle dynamics in rigid interfacial layers of polymer nanocomposites. *Journal of Applied Physics* **2021,** *130* (6), 064701.

24. Riggleman, R. A.; Douglas, J. F.; de Pablo, J. J., Tuning polymer melt fragility with antiplasticizer additives. *The Journal of Chemical Physics* **2007,** *126* (23), 234903.

25. Gong, S.; Chen, Q.; Moll, J. F.; Kumar, S. K.; Colby, R. H., Segmental Dynamics of Polymer Melts with Spherical Nanoparticles. *ACS Macro Letters* **2014,** *3* (8), 773-777.

26. Jain, S.; Goossens, J. G. P.; Peters, G. W. M.; van Duin, M.; Lemstra, P. J., Strong decrease in viscosity of nanoparticle-filled polymer melts through selective adsorption. *Soft Matter* **2008,** *4* (9), 1848-1854.

27. Moll, J. F.; Akcora, P.; Rungta, A.; Gong, S.; Colby, R. H.; Benicewicz, B. C.; Kumar, S. K., Mechanical Reinforcement in Polymer Melts Filled with Polymer Grafted Nanoparticles. *Macromolecules* **2011,** *44* (18), 7473-7477.

28. Park, J.; Bailey, E. J.; Composto, R. J.; Winey, K. I., Single-Particle Tracking of Nonsticky and Sticky Nanoparticles in Polymer Melts. *Macromolecules* **2020,** *53* (10), 3933-3939.

29. Senses, E.; Kitchens, C. L.; Faraone, A., Viscosity reduction in polymer nanocomposites: Insights from dynamic neutron and X-ray scattering. *Journal of Polymer Science* **2022,** *60* (7), 1130-1150.

30. Nath, P.; Mangal, R.; Kohle, F.; Choudhury, S.; Narayanan, S.; Wiesner, U.; Archer, L. A., Dynamics of Nanoparticles in Entangled Polymer Solutions. *Langmuir* **2018,** *34* (1), 241-249.

31. Leheny, R. L., XPCS: Nanoscale motion and rheology. *Current Opinion in Colloid & Interface Science* **2012,** *17* (1), 3-12.

32. Kim, D.; Srivastava, S.; Narayanan, S.; Archer, L. A., Polymer nanocomposites: polymer and particle dynamics. *Soft Matter* **2012,** *8* (42), 10813-10818.

33. Jhalaria, M.; Jimenez, A. M.; Mathur, R.; Tekell, M. C.; Huang, Y.; Narayanan, S.; Benicewicz, B. C.; Kumar, S. K., Long-Term Aging in Miscible Polymer Nanocomposites. *Macromolecules* **2022,** *55* (11), 4502-4515.

34. Guo, H.; Bourret, G.; Lennox, R. B.; Sutton, M.; Harden, J. L.; Leheny, R. L., Entanglement-controlled subdiffusion of nanoparticles within concentrated polymer solutions. *Physical Review Letters* **2012,** *109* (5).

35. Song, J.; Zhang, Q.; De Quesada, F.; Rizvi, M. H.; Tracy, J. B.; Ilavsky, J.; Narayanan, S.; Del Gado, E.; Leheny, R. L.; Holten-Anderse, N.; McKinley, G. H., Microscopic dynamics

underlying the stress relaxation of arrested soft materials. *Proceedings of the National Academy of Sciences of the United States of America* **2022,** *119* (30).

36. Srivastava, S.; Agarwal, P.; Mangal, R.; Koch, D. L.; Narayanan, S.; Archer, L. A., Hyperdiffusive Dynamics in Newtonian Nanoparticle Fluids. *ACS Macro Letters* **2015,** *4* (10), 1149-1153.

37. Cipelletti, L.; Manley, S.; Ball, R. C.; Weitz, D. A., Universal Aging Features in the Restructuring of Fractal Colloidal Gels. *Physical Review Letters* **2000,** *84* (10), 2275-2278.

38. Tamborini, E.; Cipelletti, L.; Ramos, L., Plasticity of a colloidal polycrystal under cyclic shear. *Physical Review Letters* **2014,** *113* (7).

39. Senses, E.; Faraone, A.; Akcora, P., Microscopic Chain Motion in Polymer Nanocomposites with Dynamically Asymmetric Interphases. *Scientific Reports* **2016,** *6*, 29326.

40. Senses, E.; Isherwood, A.; Akcora, P., Reversible Thermal Stiffening in Polymer Nanocomposites. *ACS Applied Materials & Interfaces* **2015,** *7* (27), 14682-14689.

41. Wu, D.; Ge, Y.; Li, R.; Feng, Y.; Akcora, P., Thermally Activated Shear Stiffening in Polymer-Grafted Nanoparticle Composites for High-Temperature Adhesives. *ACS Applied Polymer Materials* **2022,** *4* (4), 2819-2827.

42. Yang, S.; Hassan, M.; Akcora, P., Role of adsorbed chain rigidity in reinforcement of polymer nanocomposites. *Journal of Polymer Science, Part B: Polymer Physics* **2019,** *57* (1), 9-14.

43. Wu, D.; Weiblen, D. G.; Ozisik, R.; Akcora, P., Local Viscosity of Interfacial Layers in Polymer Nanocomposites Measured by Magnetic Heating. *ACS Applied Polymer Materials* **2020,** *2* (12), 5542-5549.

44. Cheng, C.-H.; Kamitani, K.; Masuda, S.; Uno, K.; Dechnarong, N.; Hoshino, T.; Kojio, K.; Takahara, A., Dynamics of matrix-free nanocomposites consisting of block copolymer-grafted silica nanoparticles under elongation evaluated through X-ray photon correlation spectroscopy. *Polymer* **2021,** *229*, 124003.

45. Hernández, R.; Nogales, A.; Sprung, M.; Mijangos, C.; Ezquerra, T. A., Slow dynamics of nanocomposite polymer aerogels as revealed by X-ray photocorrelation spectroscopy (XPCS). *The Journal of Chemical Physics* **2014,** *140* (2), 024909.

46. Narayanan, S.; Lee, D. R.; Hagman, A.; Li, X.; Wang, J., Particle Dynamics in Polymer-Metal Nanocomposite Thin Films on Nanometer-Length Scales. *Physical Review Letters* **2007,** *98* (18), 185506.

47. Guo, H.; Bourret, G.; Corbierre, M. K.; Rucareanu, S.; Lennox, R. B.; Laaziri, K.; Piche, L.; Sutton, M.; Harden, J. L.; Leheny, R. L., Nanoparticle Motion within Glassy Polymer Melts. *Physical Review Letters* **2009,** *102* (7), 075702.

48. Rubinstein, M., Polymer Physics. *Oxford University Press Inc.* **2003**.

49. Beaucage, G., Approximations Leading to a Unified Exponential/Power-Law Approach to Small-Angle Scattering. *Journal of Applied Crystallography* **1995,** *28* (6), 717-728.

50. Mangal, R.; Srivastava, S.; Narayanan, S.; Archer, L. A., Size-Dependent Particle Dynamics in Entangled Polymer Nanocomposites. *Langmuir* **2016,** *32* (2), 596-603.

51. Chen, R.; Kotkar, S. B.; Poling-Skutvik, R.; Howard, M. P.; Nikoubashman, A.; Conrad, J. C.; Palmer, J. C., Nanoparticle dynamics in semidilute polymer solutions: Rings versus linear chains. *Journal of Rheology* **2021,** *65* (4), 745-755.

52. Chen, R.; Poling-Skutvik, R.; Nikoubashman, A.; Howard, M. P.; Conrad, J. C.; Palmer, J. C., Coupling of Nanoparticle Dynamics to Polymer Center-of-Mass Motion in Semidilute Polymer Solutions. *Macromolecules* **2018,** *51* (5), 1865-1872.